Electronic Supplementary Information

Development of MOF-5-like ultra-microporous metal-squarate frameworks for efficient acetylene storage and separation

Hai-Peng Li,[a, b] Jia-Wen Wang,[a] and Quan-Guo Zhai [a]*

[a] Institute of New Concept Sensors and Molecular Materials, Key Laboratory of Applied Surface and Colloid Chemistry, Ministry of Education, School of Chemistry& Chemical Engineering, Shaanxi Normal University, Xi'an, Shaanxi, 710062, China.

[b] Ningxia Key Laboratory of Green Catalytic Materials and Technology, College of Chemistry and Chemical Engineering, Ningxia Normal University, Guyuan, 756000, China.

*Corresponding author

Email: zhaiqg@snnu.edu.cn (Q.-G. Zhai)

Table S1 Crystal and structure refinement data for SNNU-505-M

MOF	SNNU-505-Co	SNNU-505-Zn
CCDC number	2269216	2269215
Empirical formula	$C_{12}H_4O_{16}Co_4$	$C_{12}F_4O_{12}Zn_4$
Formula weight	639.87	663.44
Crystal system	Cubic	Cubic
Space group	*Fm-3m*	*Fm-3m*
Temperature	153(2) K	293(2) K
Wavelength	1.54178 Å	0.71073 Å
a (Å)	19.00940(10)	19.2274(6)
b (Å)	19.00940(10)	19.2274(6)
c (Å)	19.00940(10)	19.2274(6)
α (deg)	90	90
β (deg)	90	90
γ (deg)	90	90
V (Å^3)	6869.19	7108.3
Z	8	8
D_{calcd}(Mg·m^{-3})	1.237	1.241
Reflections/Unique	6622 / 372	3229 / 593
R(int)	0.0656	0.0515
Goodness-of-fit on F^2	1.161	1.204
R_1[a], wR_2 [I > 2δ (I)]	0.0687, 0.2061	0.0719, 0.2216
R_1, wR_2 (all data)	0.0751, 0.2164	0.0896, 0.2344
ρ_{fin}(max/min) (e·Å^{-3})	1.40 and -2.07	0.88 and -1.386

[a] $R_1 = \sum(|F_o|-|F_c|)/\sum|F_o|$, $wR_2 = [\sum w(F_o^2-F_c^2)2/\sum w(F_o^2)^2]^{0.5}$

Table S2 Selected bond lengths [Å] and angles [º] for SNNU-505-Zn

Zn-O	2.090(6)	Zn-F	2.166(4)
$O^{\#1}$-Zn-$O^{\#2}$	89.3(2)	$O^{\#1}$-Zn-F(1)$^{\#3}$	94.8(17)
$O^{\#2}$-Zn-F $^{\#3}$	174.3(3)	$F^{\#4}$-Zn-F	80.9
Zn $^{\#4}$-F-Zn	98.5(3)		

Symmetry codes: #1 +z,1/2-x, 1/2-y; #2 1/2-y,1/2-z, +x; #3 +y,1/2-x, 1/2-z; #4 1/2-y, +x,1/2-z.

Table S3 Selected bond lengths [Å] and angles [º] for SNNU-505-Co

Co-O(1)	2.123(5)	Co-O(2)	2.071(5)
O(2)-Co-O(2)$^{\#1}$	87.04(16)	O(2)-Co-O(1)$^{\#3}$	95.08(17)
O(2)$^{\#1}$-Co-O(1)$^{\#3}$	177.1(3)	O(1)$^{\#3}$-Co-O(1)$^{\#4}$	82.7(3)
Co$^{\#3}$-O(1)-Co	96.8(3)		

Symmetry codes: #1 1-y,1-z, +x; #3 1/2-x, +y, 1/2-z; #4 1/2-x, 3/2-y, +z.

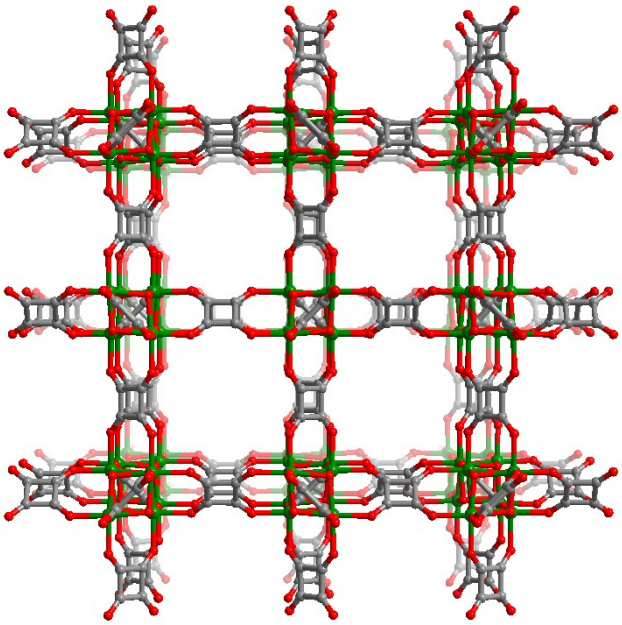

Figure S1. The three-dimensionalcrystal structures of SNNU-505-M.

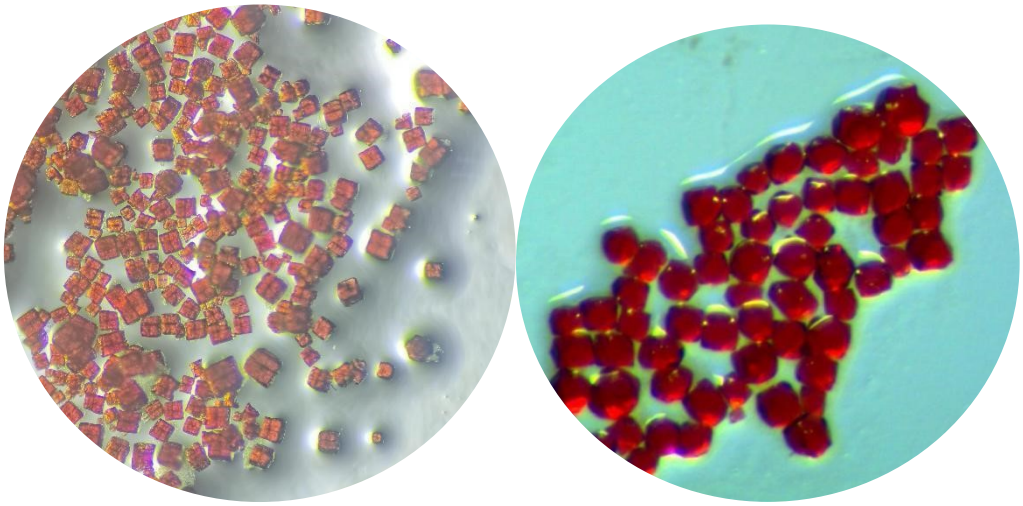

(a) **(b)**

Figure S2. The single crystal picture for SNNU-505-Zn (a) and SNNU-505-Co (b).

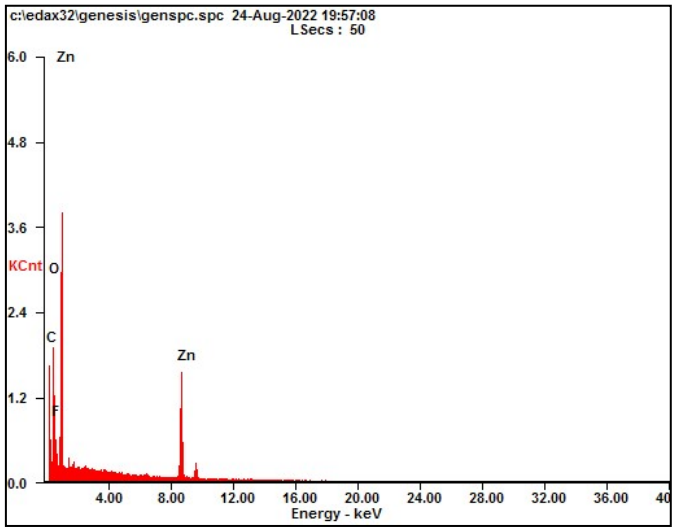

Element	*Wt %*	*At %*
C K	39.53	61.75
O K	20.75	24.33
F K	03.60	03.55
ZnK	36.13	10.37

Figure S3. The EDS results for SNNU-505-Zn.

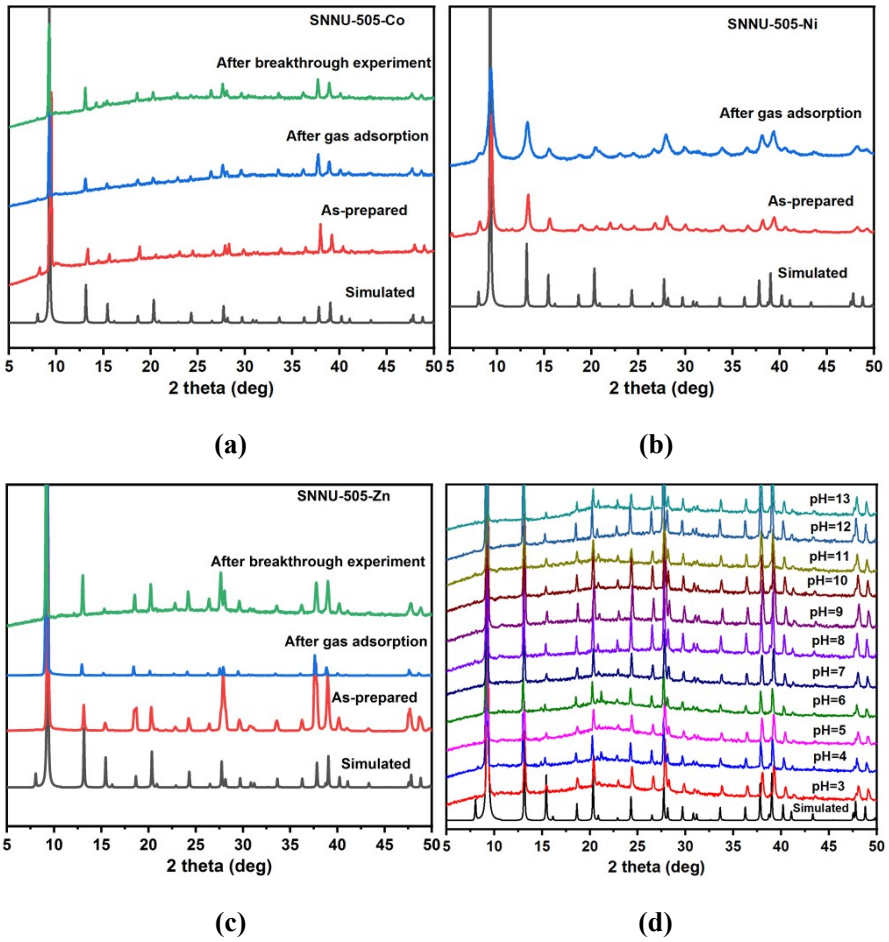

Figure S4. PXRD patterns for SNNU-505-M.

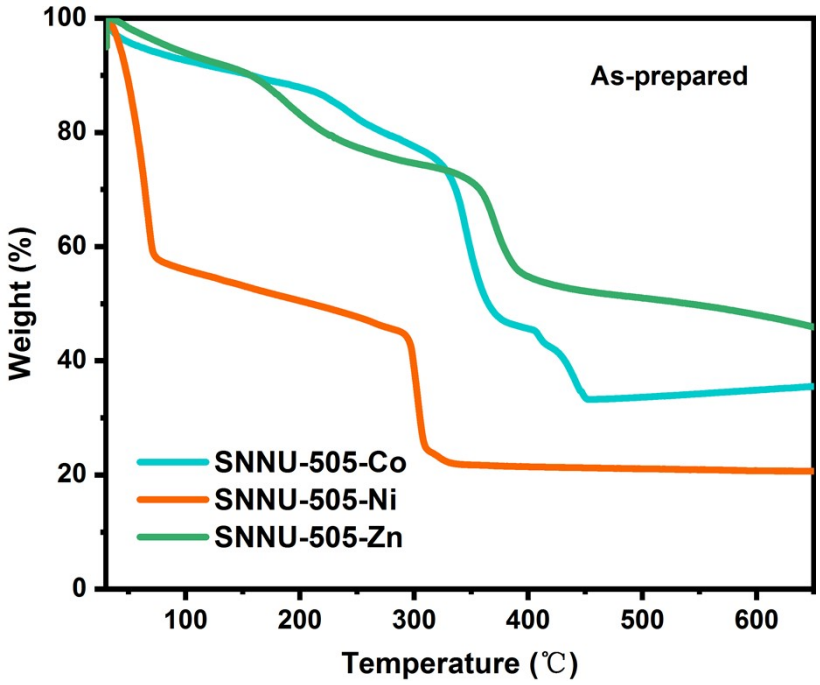

(a)

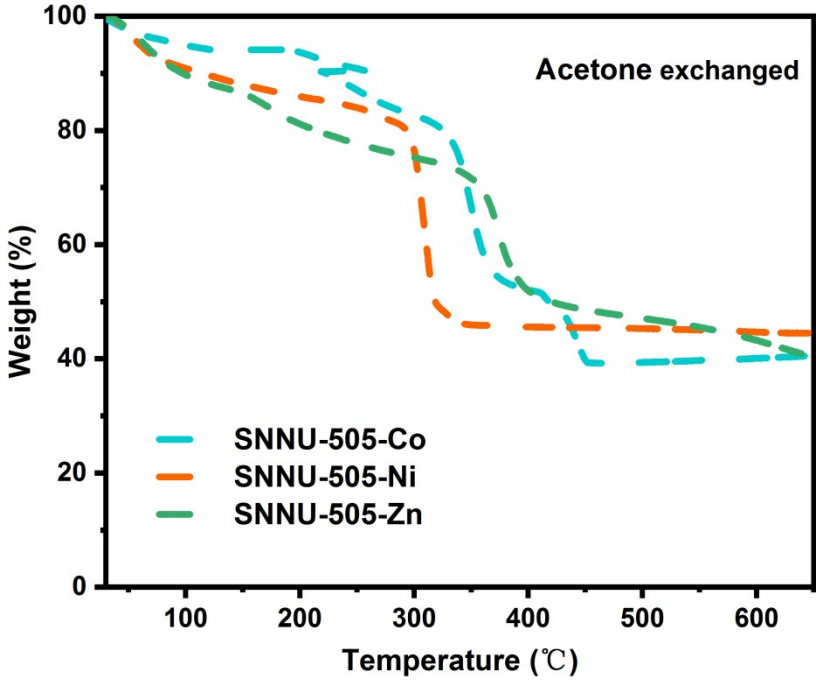

(b)

Figure S5. The TGA curve for SNNU-505-M based on before and after solvent exchange.

Estimation of the isosteric heats of gas adsorption. The isosteric enthalpy of adsorption ($-Q_{st}$) for C_2H_2, C_2H_4 and CO_2 can be calculated via using virial-type expression model based on the gas adsorption isotherms under 273 K and 298 K.[S1]

$$\ln P = \ln N + \frac{1}{T}\sum_{i=0}^{m} a_i N^i + \sum_{i=0}^{m} b_i N^i \quad (1)$$

$$Qst = -R\sum_{i=0}^{m} a_i N^i \quad (2)$$

IAST calculation. Based on the pure gas uptake isotherms of SNNU-505-M, the selectivity values of equimolar mixed C_2H_2/C_2H_4 and C_2H_2/CO_2 were simulated using the ideal adsorbed solution theory (IAST),[S2] and found that the single-site langmuir-freundlich (LF) equation was the most suitable for the experimental pure isotherms of CO_2, C_2H_2 and C_2H_4.

$$q = q_{m1} * \frac{b_1 * p^{1/n_1}}{1 + b_1 * p^{1/n_1}} \quad (3)$$

The adsorption selectivity was defined as:

$$s_{A/B} = \frac{x_A / y_A}{x_B / y_B} \quad (4)$$

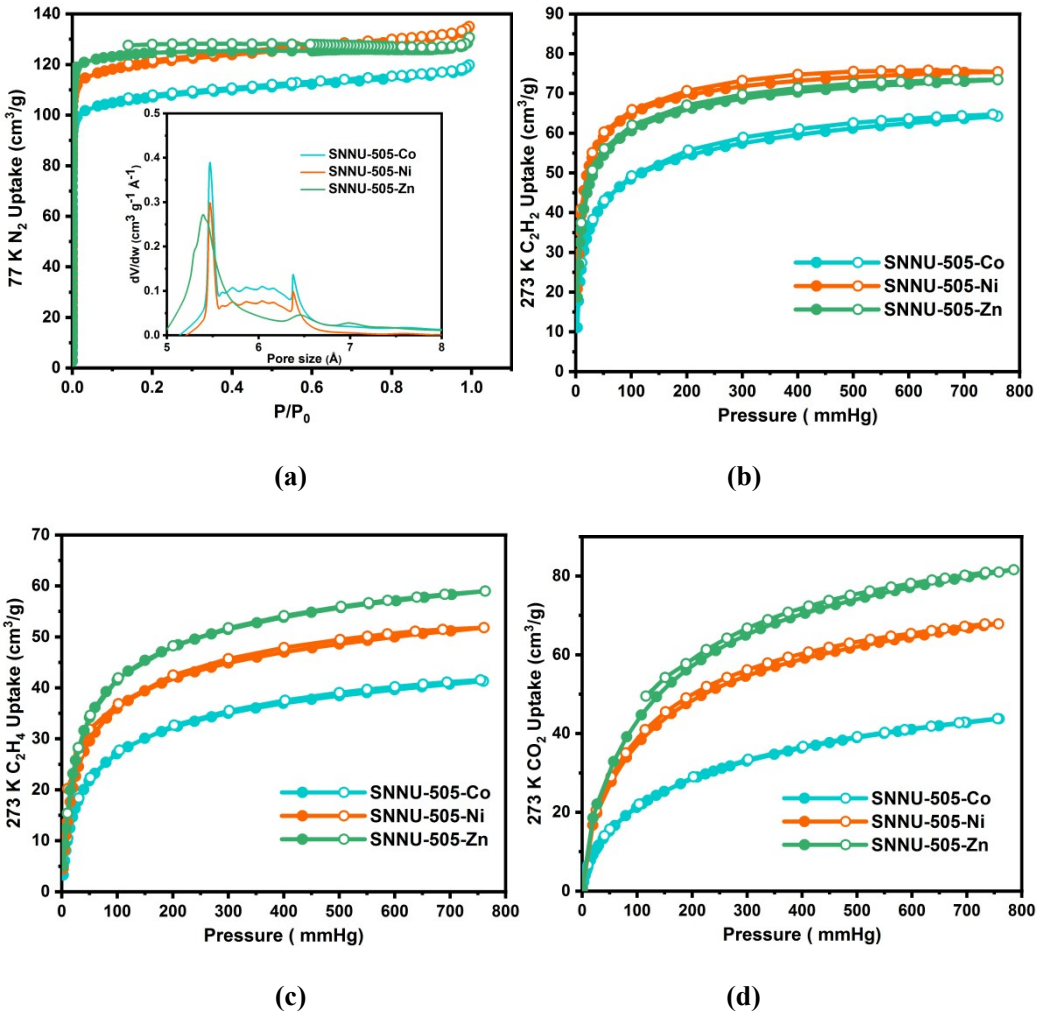

Figure S6. The adsorption and desorption isotherms for SNNU-505-M, (a) N_2 at 77 K for SNNU-505-Zn; and the C_2H_2 (b), C_2H_4 (c), CO_2 (d) adsorption isotherms for SNNU-505-M.

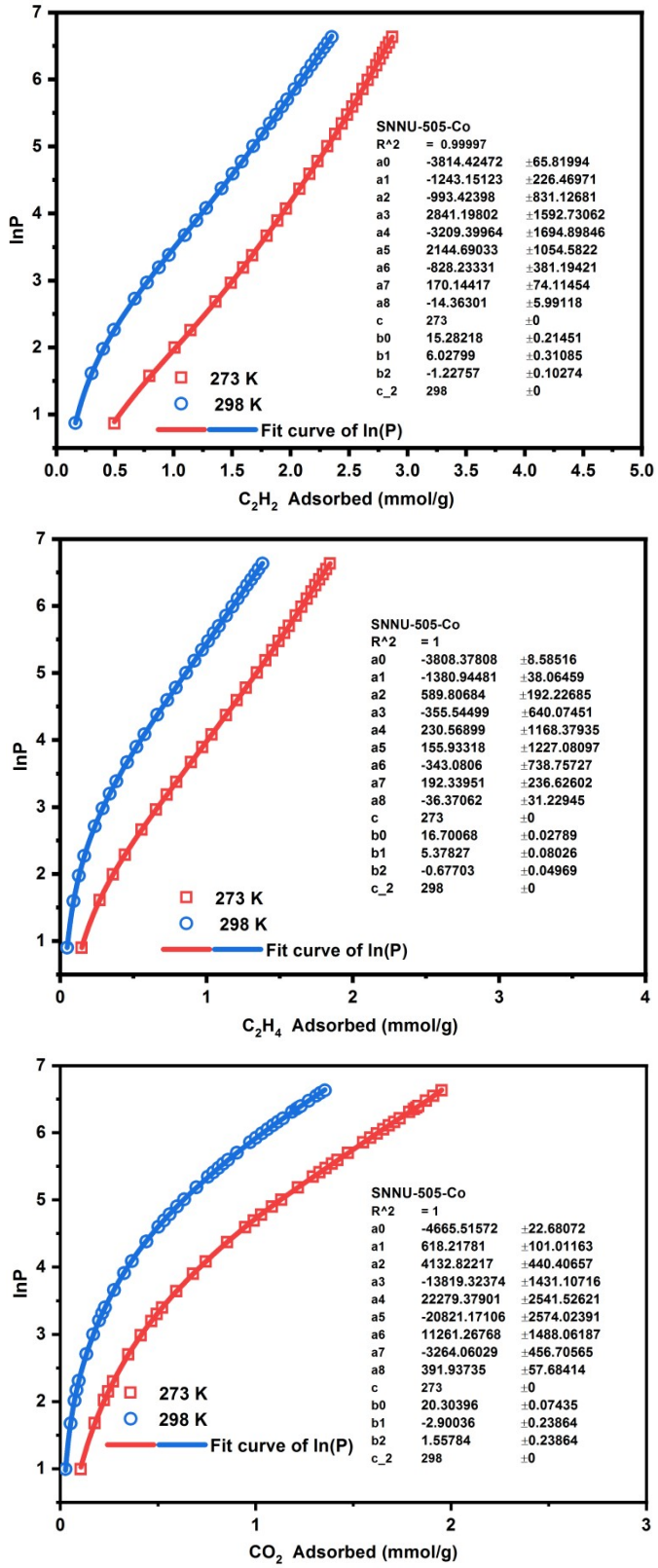

Figure S7. Fitted gas adsorption isotherms of SNNU-505-Co measured at 273 K and 298 K.

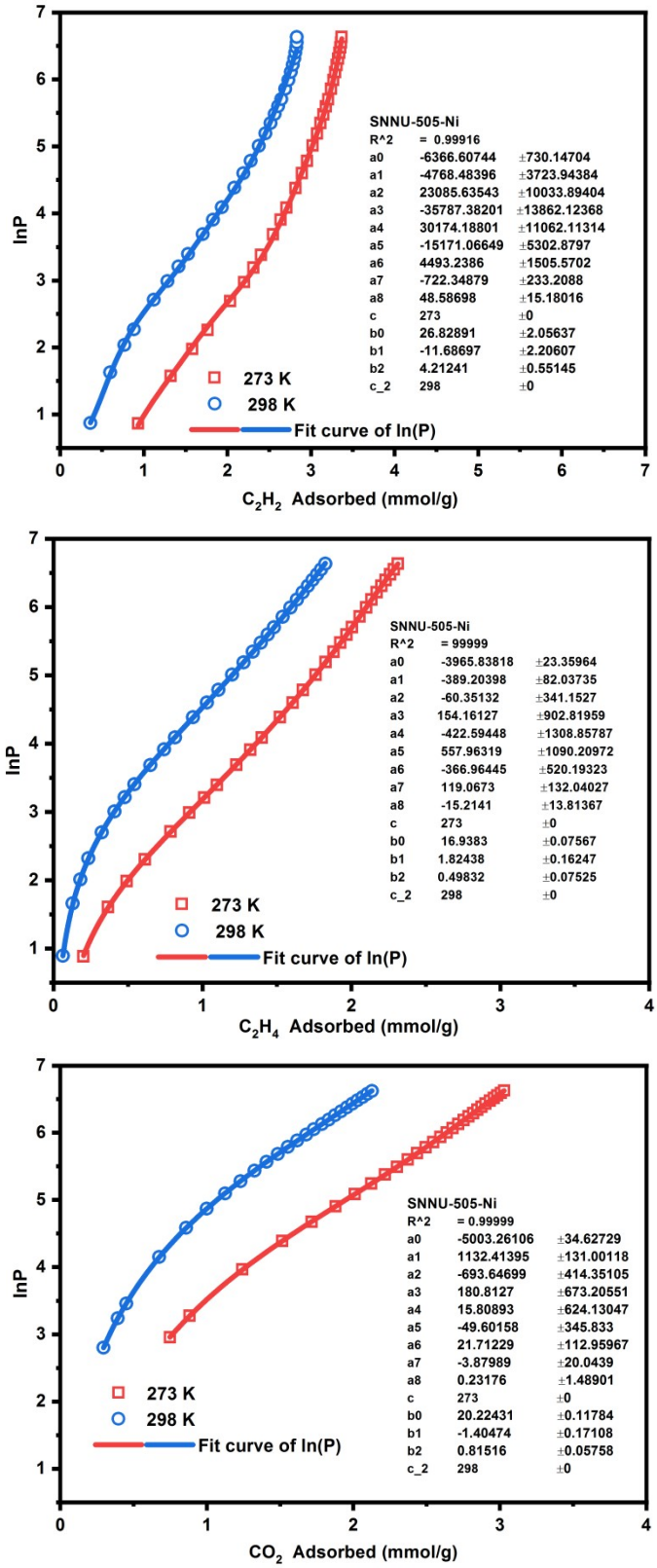

Figure S8. Fitted gas adsorption isotherms of SNNU-505-Ni measured at 273K and 298K.

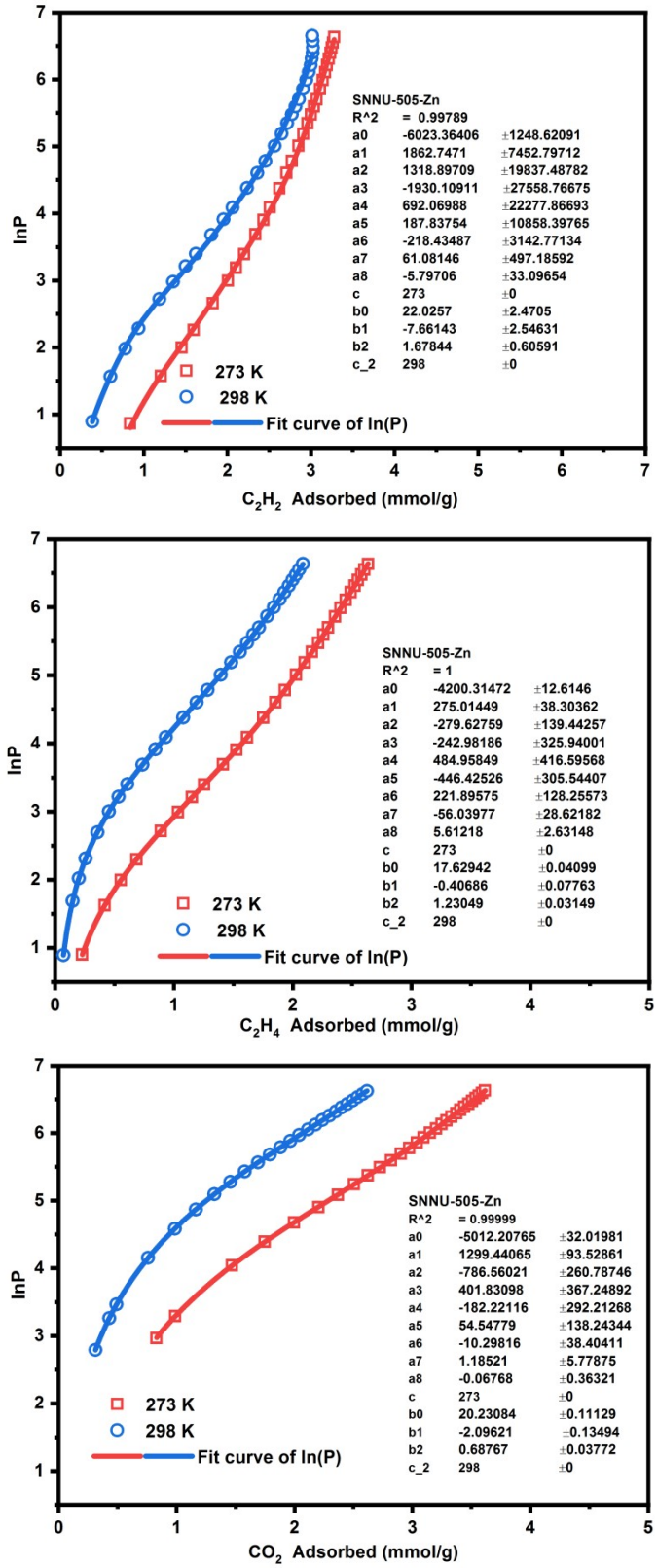

Figure S9. Fitted gas adsorption isotherms of SNNU-505-Zn measured at 273K and 298K.

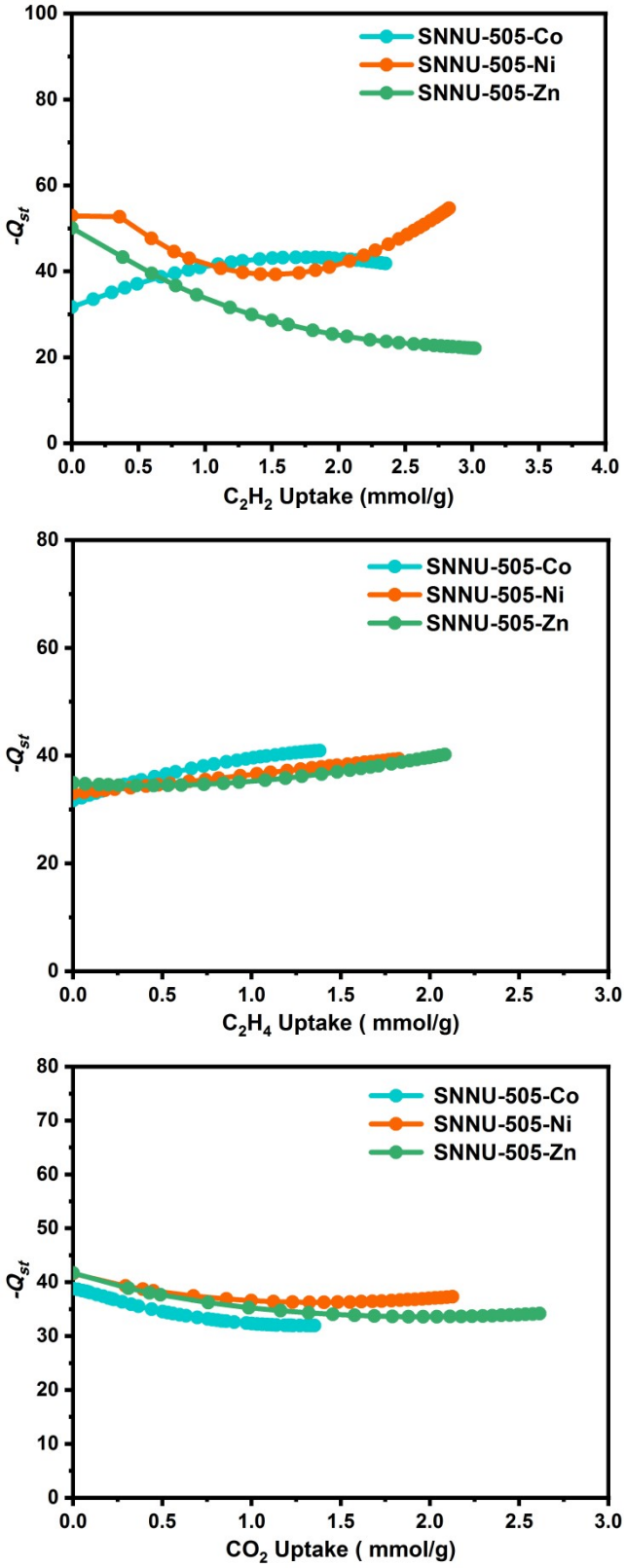

Figure S10. The isosteric heat of adsorption ($-Q_{st}$) of C_2H_2, C_2H_4, and CO_2 for SNNU-505-M.

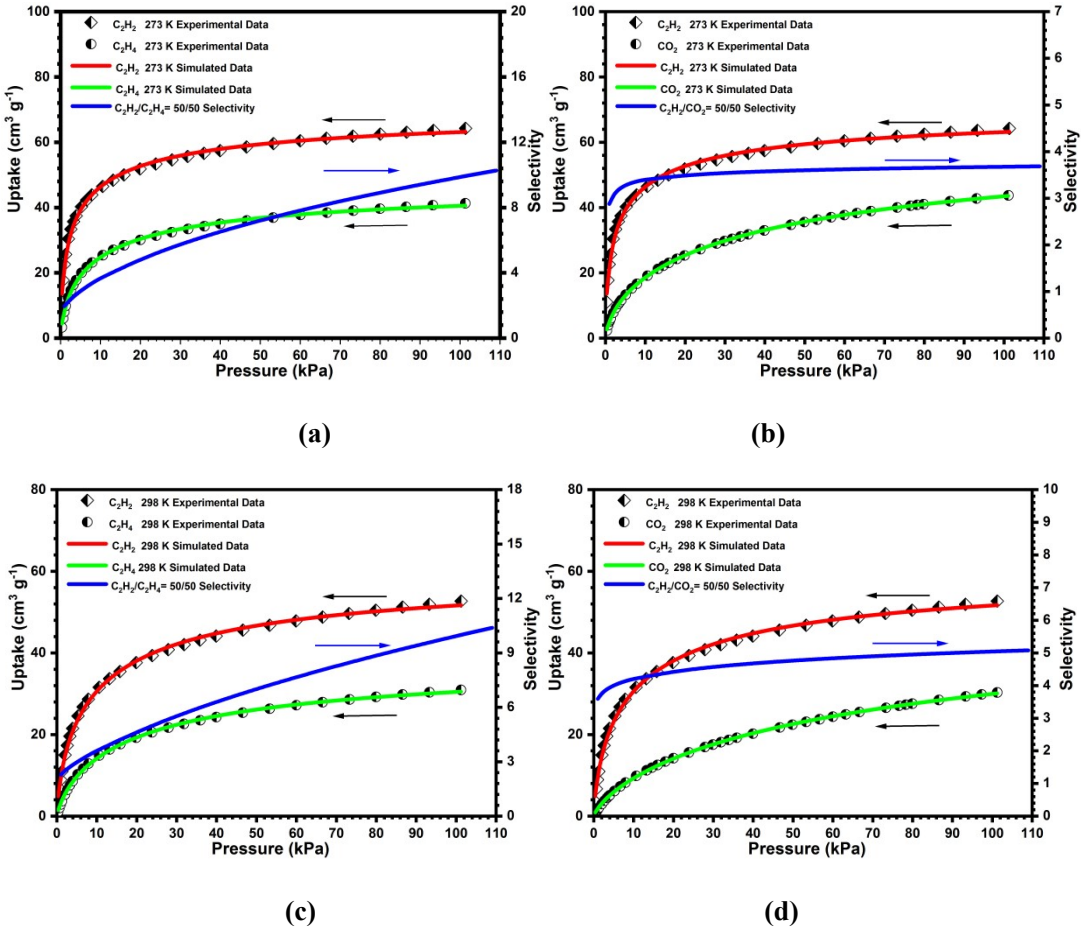

Figure S11. Comparison of experimental isotherms and simulated isotherms (Left Y axis), and mixture adsorption selectivity predicted by IAST (Right Y axis) of SNNU-505-Co for equimolar binary-mixture: (a) C_2H_2/C_2H_4 at 273 K; (b) C_2H_2/CO_2 at 273 K; (c) C_2H_2/C_2H_4 at 298 K; (d) C_2H_2/CO_2 at 298 K.

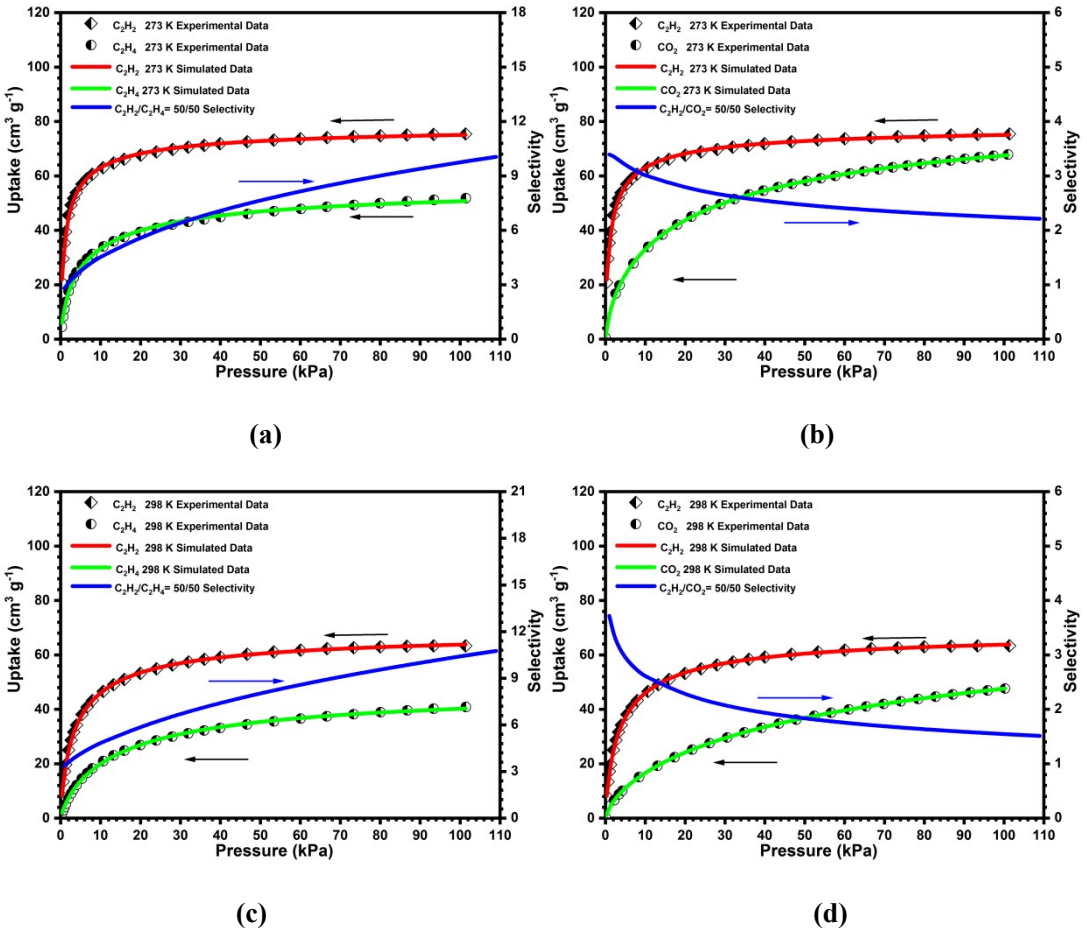

Figure S12. Comparison of experimental isotherms and simulated isotherms (Left Y axis), and mixture adsorption selectivity predicted by IAST (Right Y axis) of SNNU-505-Ni for equimolar binary-mixture: (a) C_2H_2/C_2H_4 at 273 K; (b) C_2H_2/CO_2 at 273 K; (c) C_2H_2/C_2H_4 at 298 K; (d) C_2H_2/CO_2 at 298 K.

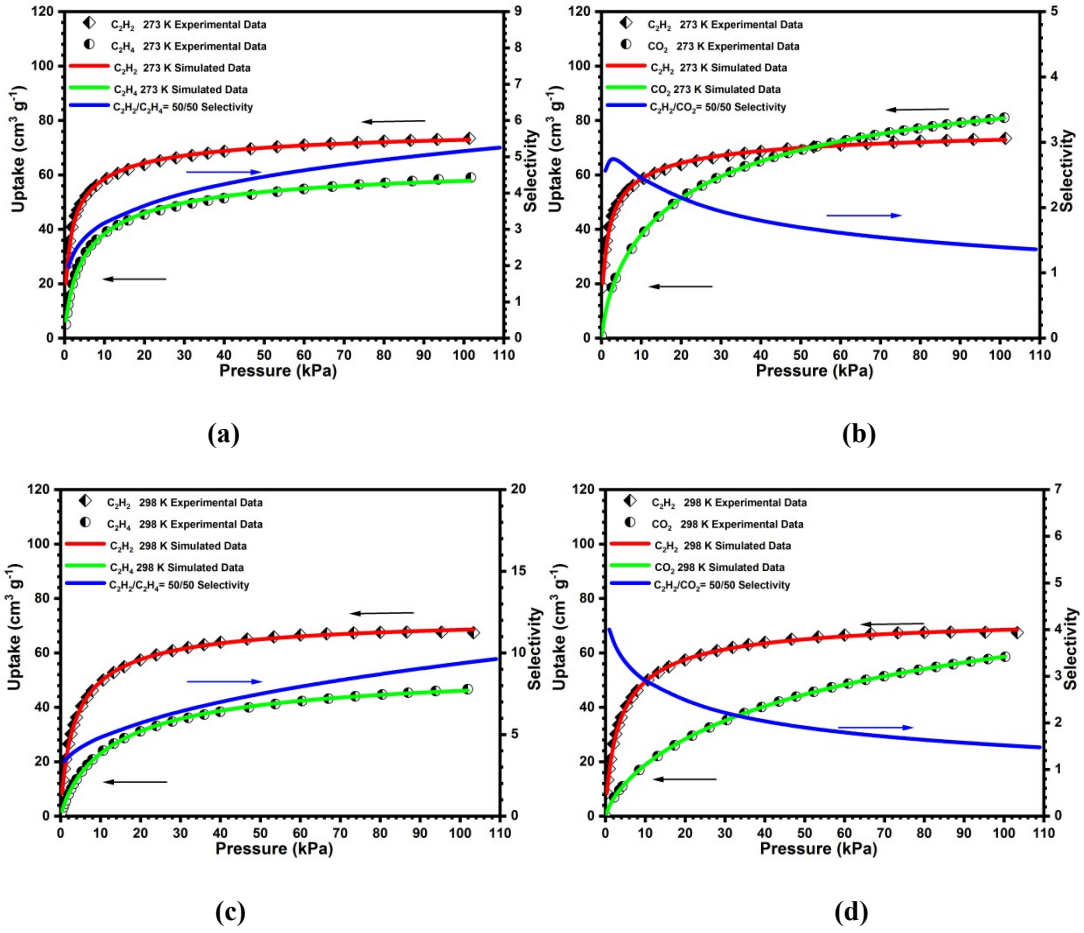

Figure S13. Comparison of experimental isotherms and simulated isotherms (Left Y axis), and mixture adsorption selectivity predicted by IAST (Right Y axis) of SNNU-505-Zn for equimolar binary-mixture: (a) C_2H_2/C_2H_4 at 273 K; (b) C_2H_2/CO_2 at 273 K; (c) C_2H_2/C_2H_4 at 298 K, (d) C_2H_2/CO_2 at 298 K.

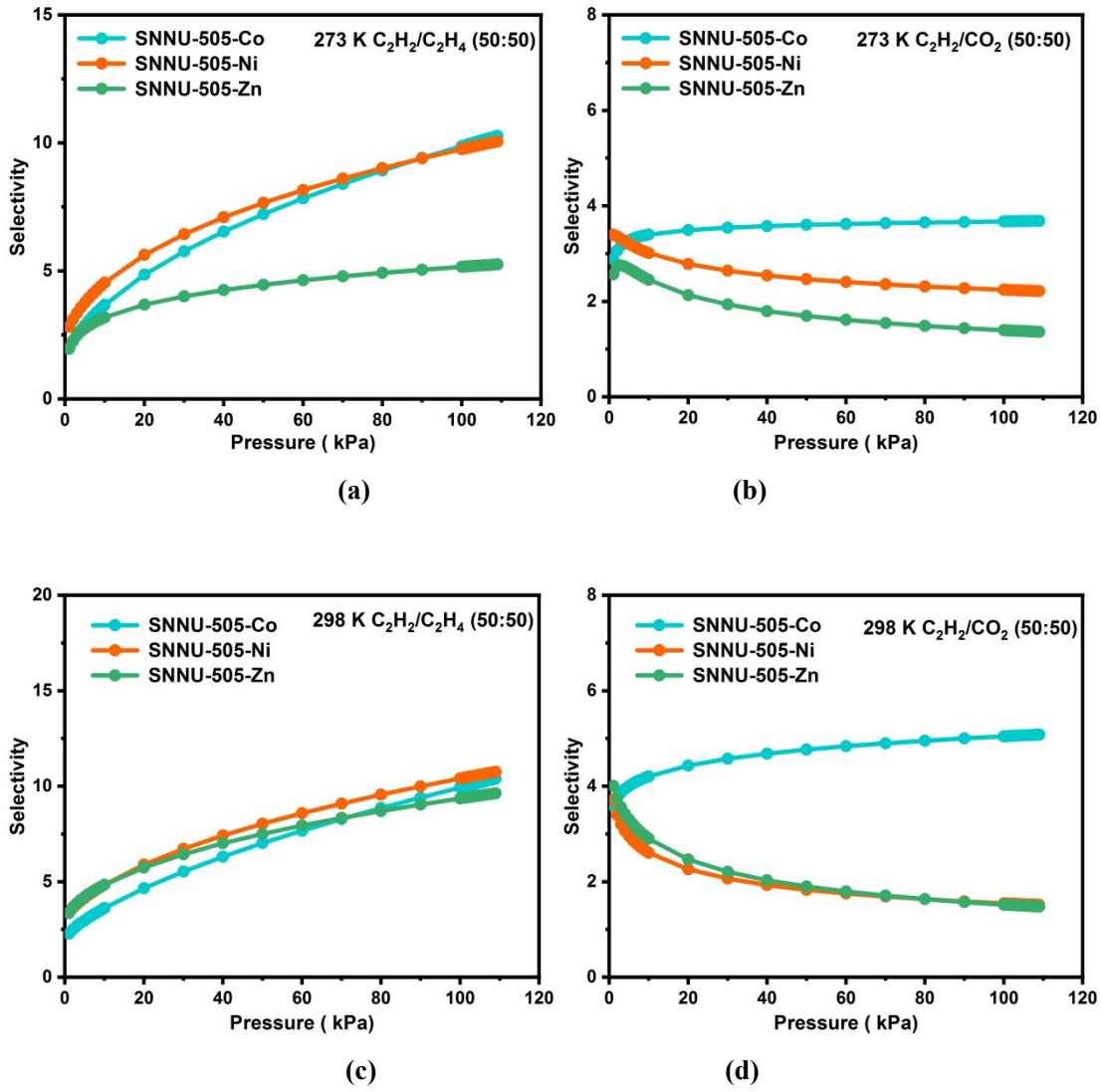

Figure S14. The selectivity of C_2H_2/C_2H_4 and C_2H_2/CO_2 predicted by IAST for SNNU-505-M. (a-b) at 273 K; (c-d) at 298 K.

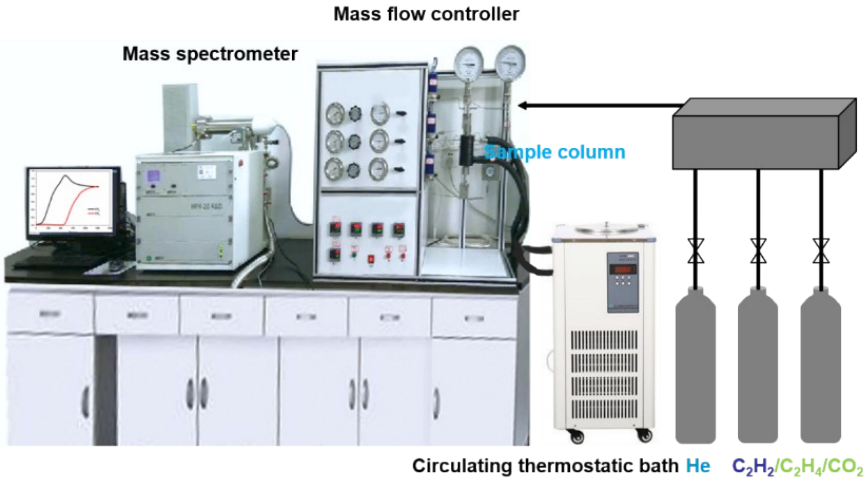

Figure S15. Schematic illustration of the apparatus for the breakthrough experiments.

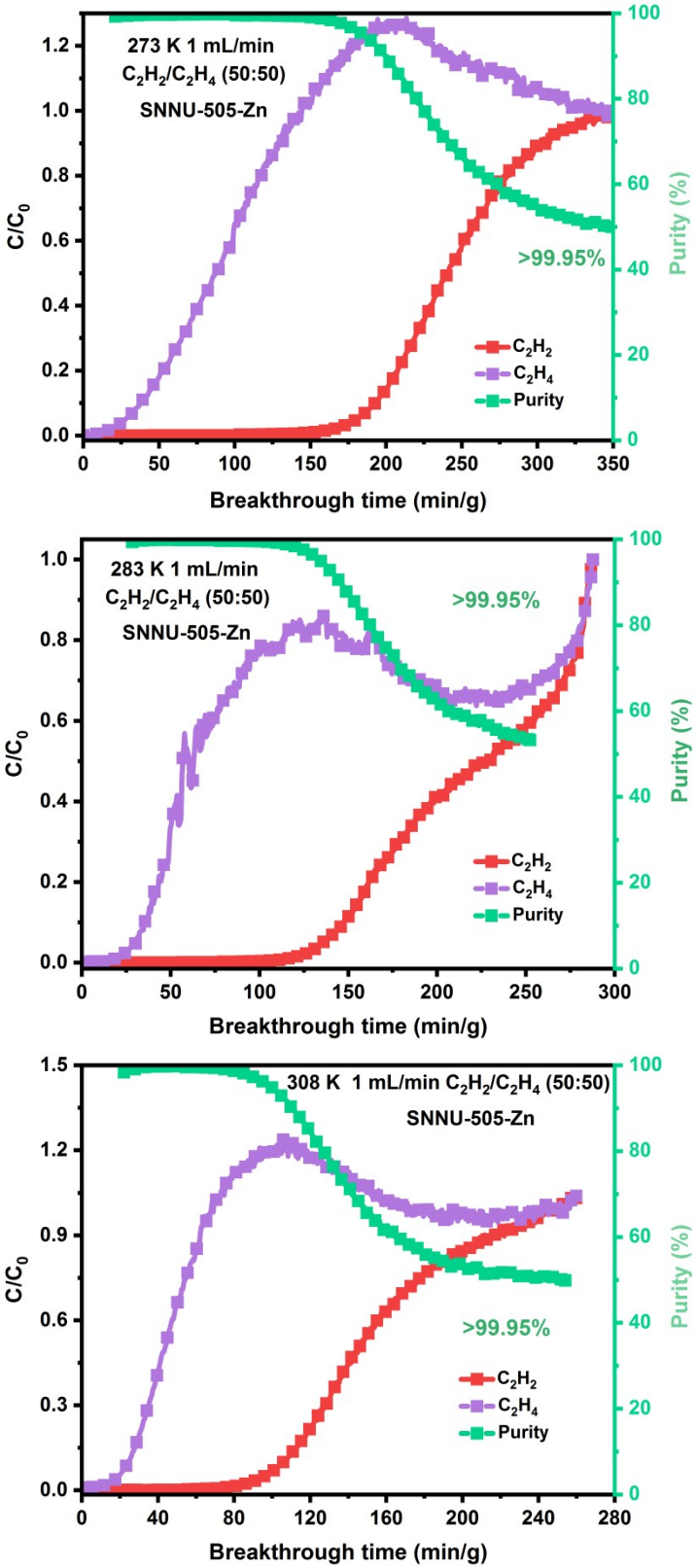

Figure S16. The C_2H_2/C_2H_4 breakthrough curve for SNNU-505-Zn at different temperatures and the total flow of 1 mL/min.

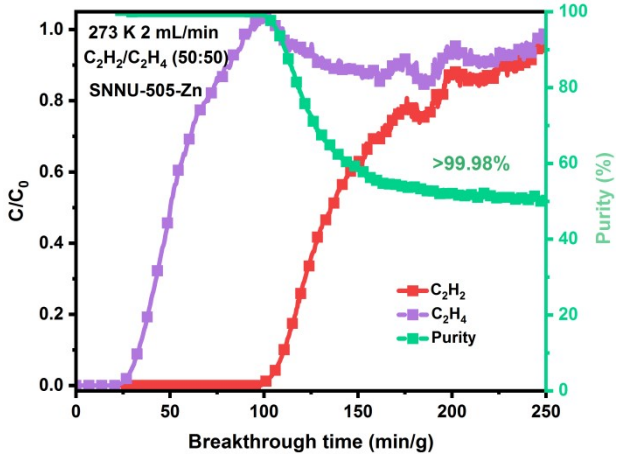

(a)

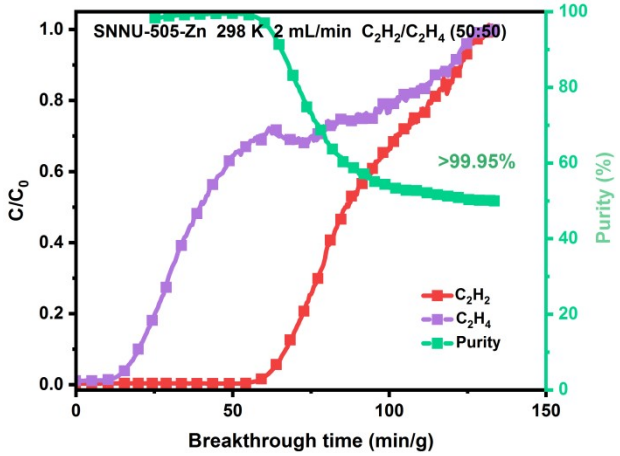

(b)

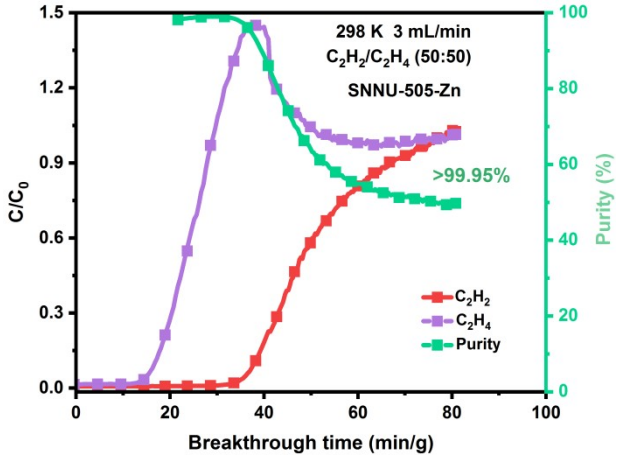

(c)

Figure S17. The breakthrough curves of C_2H_2/C_2H_4 gas mixtures for SNNU-505-Zn. (a) and (b) the breakthrough curve collected under different temperature and the total flow of 2 mL/min; (c) the breakthrough curve at 298 K and the total flow of 3 mL/min.

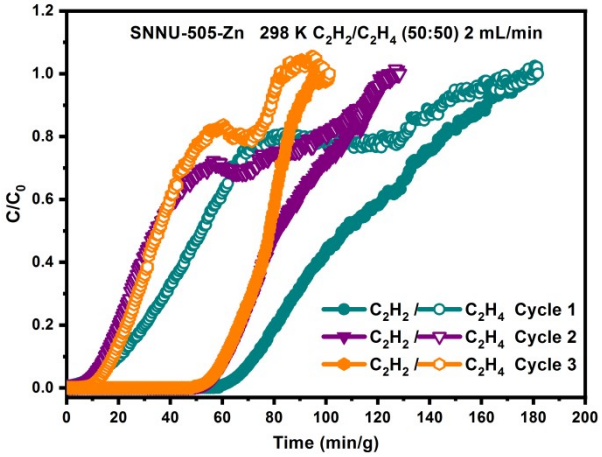

Figure S18. The C_2H_2/C_2H_4 cycle breakthrough experiment for SNNU-505-Zn.

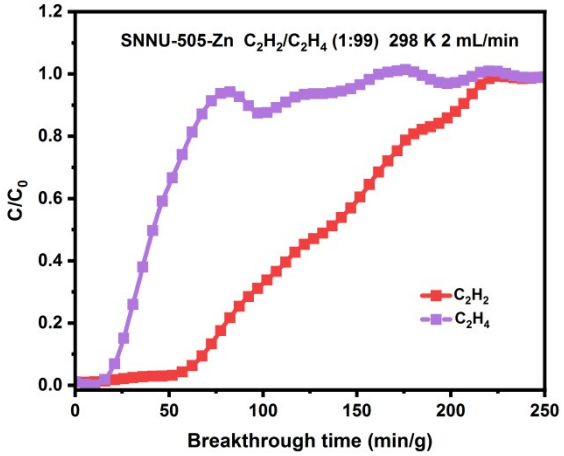

Figure S19. The breakthrough curves of C_2H_2/C_2H_4 (1:99) gas mixtures for SNNU-505-Zn.

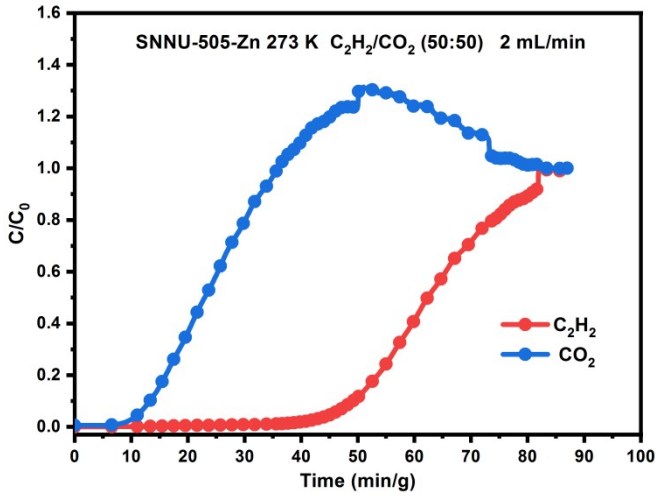

Figure S20. The C_2H_2/CO_2 (50:50) breakthrough curves for SNNU-505-Zn at 273 K.

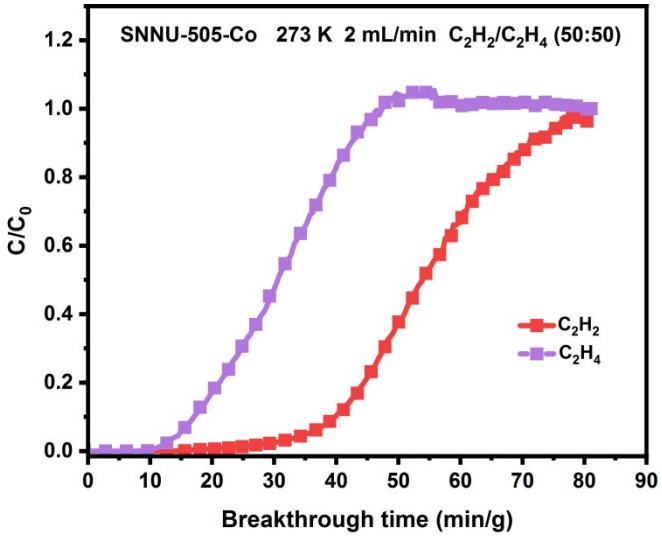

(a)

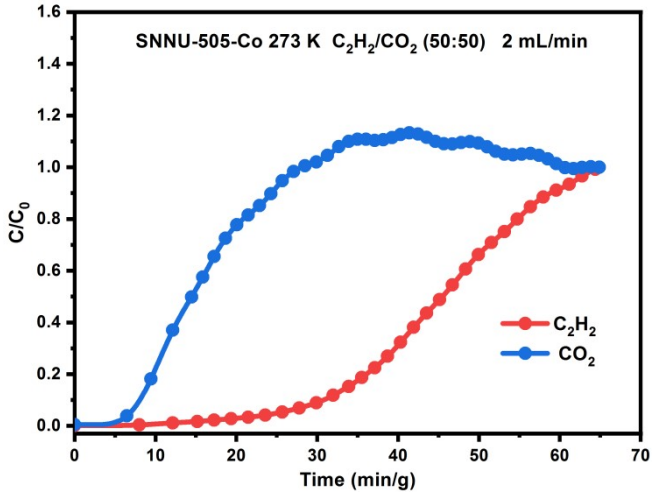

(b)

Figure S21. The breakthrough curves for SNNU-505-Co at 273 K and the total flow of 2 mL/min. (a) the C_2H_2/C_2H_4(50:50) breakthrough curve; (b) the C_2H_2/CO_2(50:50) breakthrough curve.

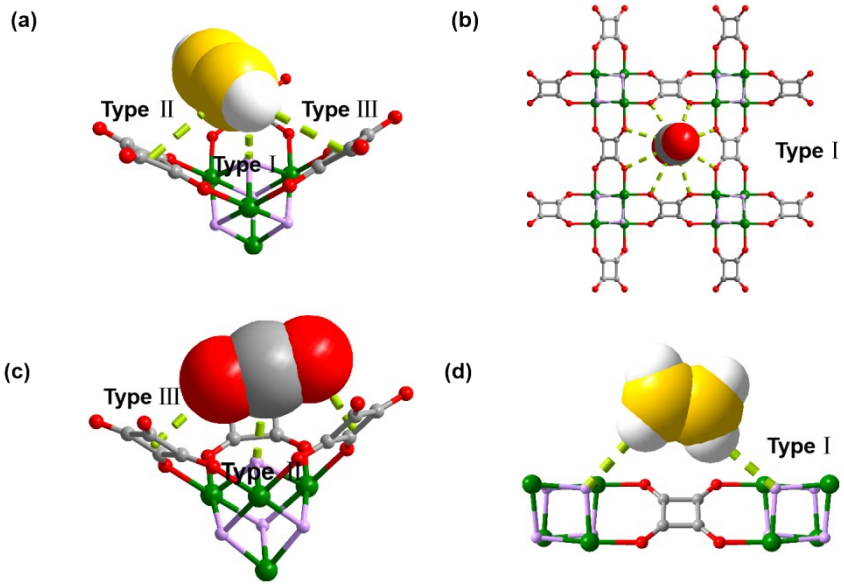

Figure S22. C_2H_2, C_2H_4 and CO_2 binding sites in SNNU-505-Zn absorbents determined by GCMC simulation.

Reference

[S1] Rowsell, J. L. C.; Yaghi, O. M. Effects of Functionalization, Catenation, and Variation of the Metal Oxide and Organic Linking Units on the Low Pressure Hydrogen Adsorption Properties of Metal-Organic Frameworks. *J. Am. Chem. Soc*. **2006**, 128, 1304-1315.

[S2] Myers, A. L.; Prausnitz, J. M. Thermodynamics of Mixed-Gas Adsorption. *AIChE J*. **1965**, 11, 121-127.

[S3] Rappe, A. K.; Goddard, W. A. Charge Equilibration for Molecular Dynamics Simulations. *J. Phys. Chem*., **1991**, 95, 3358-3363.